CITATION

Riser, S.C., J. Anderson, A. Shcherbina, and E. D'Asaro. 2015. Variability in near-surface salinity from hours to decades in the eastern North Atlantic: The SPURS region. *Oceanography* 28(1):66–77, http://dx.doi.org/10.5670/oceanog.2015.11.

DOI

http://dx.doi.org/10.5670/oceanog.2015.11

Variability in
Near-Surface Salinity
from Hours to Decades in
the Eastern North Atlantic:
The SPURS Region

By Stephen C. Riser, Jessica Anderson,
Andrey Shcherbina, and Eric D'Asaro

6–12 hours at surface to
transmit data to satellite

Total cycle
time – 10 days

Descent to depth – 6 hours

Temperature
and salinity
profile recorded
during ascent –
6 hours

1,000 m – drift approx. 9 days

Float descends
to begin profile
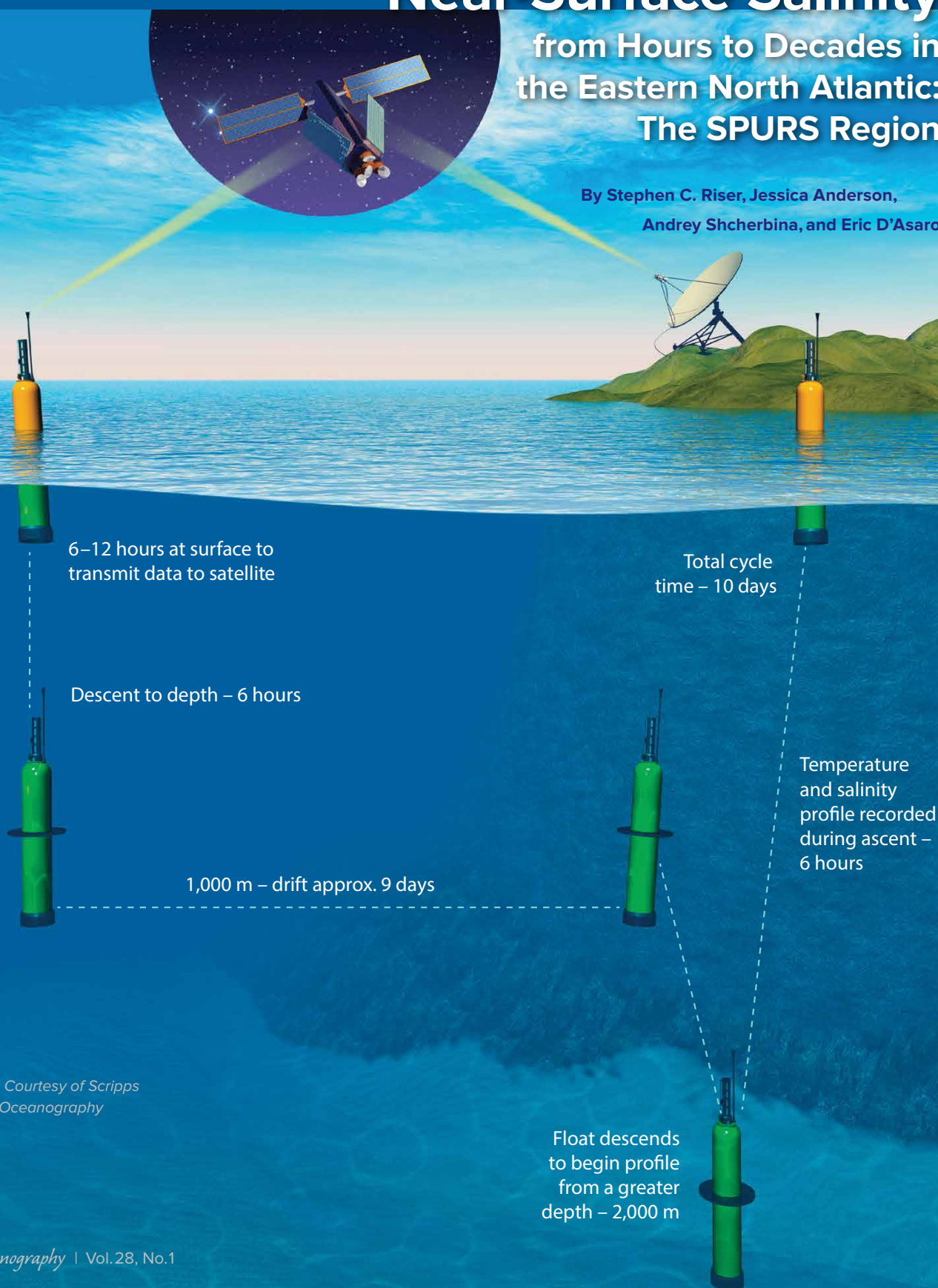from a greater
depth – 2,000 m

Image credit: Courtesy of Scripps
Institution of Oceanography

> By comparing the SPURS measurements to observations in the area from previous decades, we examine variability at time scales ranging from a few hours (mostly consisting of rainfall-driven decreases in salinity) to diurnal cycles in temperature and salinity, seasonal variability and the annual cycle, and finally to decadal-scale changes.

ABSTRACT. We examine the variability of near-surface salinity in a 10° × 10° region of the eastern North Atlantic, the location of the first part of the Salinity Processes in the Upper-ocean Regional Study (SPURS-1). The data used were collected over a two-year period, largely by a group of two types of profiling floats equipped with sensors that record high-resolution temperature and salinity measurements in the upper few meters of the water column. By comparing the SPURS-1 measurements to observations in the area from previous decades, we examine variability at time scales ranging from a few hours (mostly consisting of rainfall-driven decreases in salinity) to diurnal cycles in temperature and salinity, seasonal variability and the annual cycle, and finally to decadal-scale changes. The relationship of near-surface salinity to the hydrological cycle suggests a continuous spectrum of variability in this cycle from hours to decades.

INTRODUCTION

The ocean covers nearly three-quarters of Earth's surface and thus plays a central role in modulating the planet's climate. The ocean is responsible for influencing large-scale wind patterns and transporting heat and freshwater. And, given its fluid nature, the ocean is a location where properties derived from air-sea or land-sea exchanges can be mixed from the sea surface into the depths, then carried for long distances. As a repository for over 90% of the water on the planet, the ocean plays a central role in determining the characteristics of the hydrological cycle, with ocean salinity as an important part. However, until recent decades, ocean salinity was relatively poorly observed due to the difficulty of measuring it with sufficient accuracy and precision for detailed scientific analyses.

To improve understanding of the processes leading to the observed distribution of salinity in the ocean, the Salinity Processes in the Upper-ocean Regional Study (SPURS), sponsored by the National Aeronautics and Space Administration (NASA), examined salinity in a relatively small patch of the eastern North Atlantic in the fall of 2012 (SPURS-1). This multi-investigator program deployed a large collection of new and novel instrumentation, including a number of autonomous floats and gliders. We analyzed these observations in conjunction with regional sea surface salinity data acquired by the Aquarius/SAC-D satellite. In this paper, we describe observations of near-surface salinity variability collected by two types of profiling floats deployed during SPURS-1.

GLOBAL AND LOCAL BACKGROUND CONDITIONS

To put the observations from the SPURS-1 region in context, we begin by estimating the large-scale mean geostrophic ocean circulation near the sea surface using Argo float data collected from 2005–2012 (Figure 1a, constructed using the methodology of Gray and Riser, 2014). The major ocean gyres are evident in each ocean basin, with westward-intensified anticyclonic circulation ubiquitous in the subtropics. This can clearly be seen in the North Atlantic, with an intense Gulf Stream (manifested as the crowded contours along the western edge of the basin) flowing northward along the North American coast and a weaker interior return flow. In the greater SPURS-1 region (shown by the 10° × 10° gray square in Figure 1a), the flow near the sea surface is generally to the south and southwest, eventually returning to the west along the islands bounding the Caribbean. An examination of salinity near the sea surface over the globe (Figure 1b, as measured by the Aquarius/SAC-D satellite during May 2013) shows a region of relatively high salinity in the eastern portion of each of the major subtropical gyres of the world's ocean basins. In the eastern North Atlantic SPURS-1 region, the surface salinities are some of the

highest observed anywhere in the world ocean, often exceeding 37 psu (practical salinity units; in its modern definition, using the Practical Salinity Scale of 1978, salinity is dimensionless, but in an attempt to be consistent with measurements from previous eras, the values of salinity are often quoted in psu). These regions of high subtropical surface salinity generally coincide with areas of high net evaporation (as shown in Figure 1c) and Ekman convergence. The high values of net evaporation in these regions remove freshwater from the sea surface, leaving salt behind and thus increasing surface salinity, because salinity can roughly be thought of as the number of grams of salt dissolved in a kilogram of seawater. Overall, the high visual correlation between surface salinity and net evaporation suggests a plausible cause-effect relationship between these factors at the largest spatial scales.

Although the views of the ocean surface shown in Figure 1 are useful for discerning general properties, they are by nature heavily smoothed and cannot give an indication as to what the distribution of variables on smaller scales might be. To examine properties inside the 10° × 10° SPURS-1 region in more detail, we show the sea surface salinity in the region for September 2013, as measured by Aquarius (Figure 2a), and sea surface temperature for mid-September 2013, estimated from a number of satellite-based sources (Figure 2b). As these figures demonstrate, there is a considerable degree of structure across the greater SPURS-1 region. The salinity values are uniformly higher than for nearly any other region of the open ocean, with a band of extremely high surface salinity (values approaching 38 psu) crossing the region between 24°N and 28°N. The sea surface temperature changes by more than 4°C from northeast to southwest across the region.

Large-scale processes such as precipitation and evaporation or the ubiquitous equator-to-pole temperature gradient cannot alone explain the near-surface structure shown in Figure 2a and 2b. It is clear that turbulent eddies, advection by the large-scale circulation (Figure 1a), and vertical processes not visible in Figure 2 must also play important roles in determining salinity and temperature fields near the sea surface. Our lack of understanding of the nature of these factors was the major motivation for carrying out SPURS; it is our group's task to better discern the details of the processes that set the distributions shown in Figure 2, particularly the sea surface salinity.

FLOAT TECHNOLOGY AND METHODOLOGY

Our contributions to SPURS-1 result from observations collected by two types of profiling floats (Figure 3). The first type (the two left panels in the figure) is
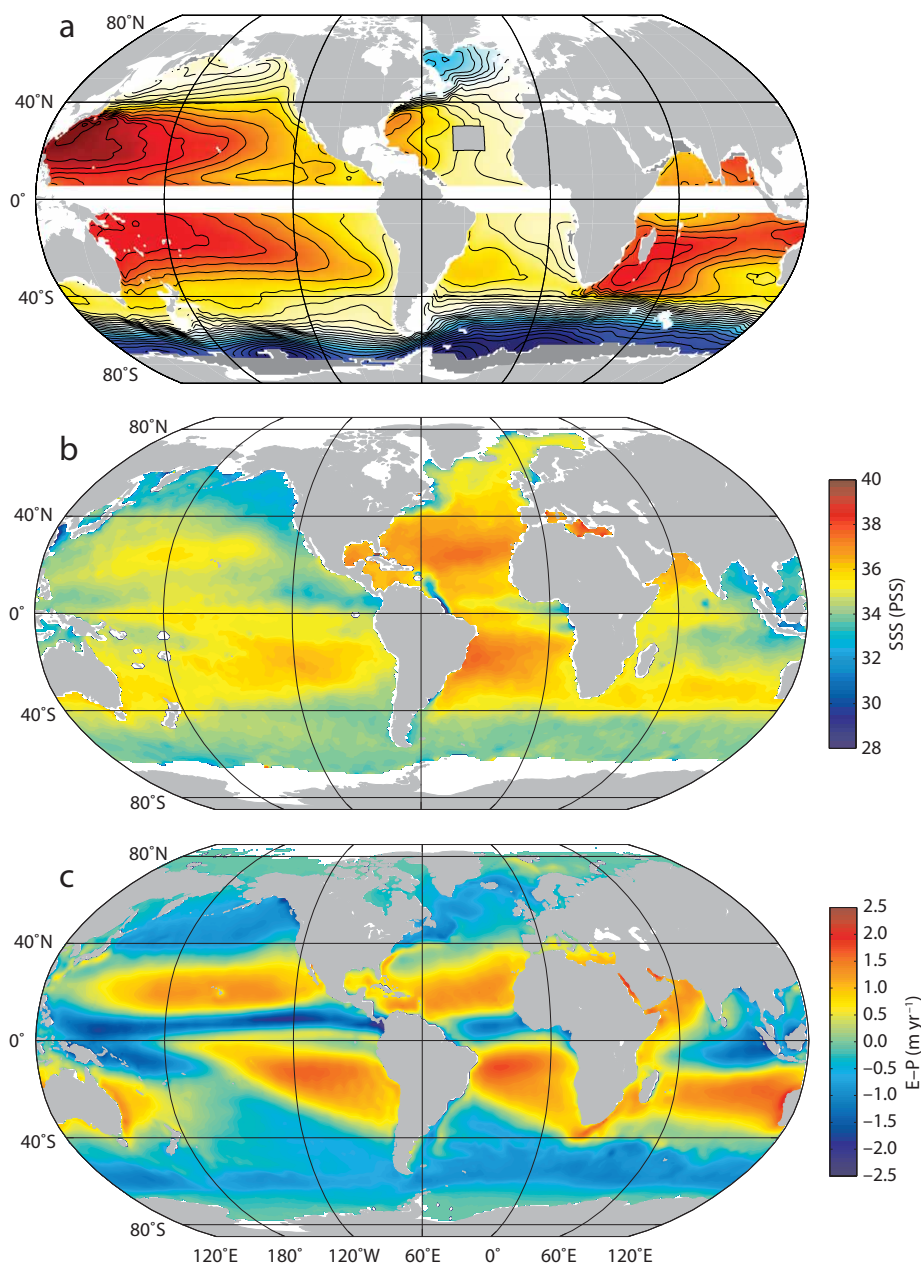

Figure 1. (a) Absolute geostrophic pressure at a depth of 5 m for the world ocean, constructed using the methodology of Gray and Riser (2014). Red areas denote high geostrophic pressure, and blue areas denote lows. Geostrophic flow is along geostrophic pressure contours (the contour interval is 10 dynamic centimeters, where 1 dynamic centimeter = 10 m² s⁻²). (b) Salinity at the sea surface as measured by the Aquarius/SAC-D satellite for May 2013. (c) Evaporation minus precipitation at the sea surface, from Schanze et al. (2010).

an APEX profiling float, constructed at the University of Washington from components purchased from Teledyne/Webb Corporation. In addition to the usual Sea-Bird conductivity-temperature-depth (CTD) sensor, each of these floats also carried a second surface temperature and salinity sensor (STS) designed to provide high-resolution (5–10 cm) measurements near the sea surface, and a broadband hydrophone capable of collecting acoustic information that can be used to estimate wind speed and rainfall (as was done by Riser et al., 2008; results of the acoustic measurements are discussed by Yang et al., 2015, in this issue). The STS unit is useful here because normal APEX floats, such as those used in the Argo program, typically shut off their CTD units at depths of 3–5 m to avoid biological fouling of the CTD during the long deployments (four to six years) that are common for Argo floats. Unlike the main CTD unit, the STS is unpumped and carries no biocide, thus allowing the possibility of biological fouling of the sensors, which can affect sensor stability. However, the main CTD (a stable, pumped unit with a biocide) and the STS are both operative between 30 m and 5 m depths, so that any STS sensor drift can be removed by comparing those data to the main CTD data after each profile. Sixteen of these STS-equipped APEX floats were deployed during SPURS-1, with the floats projected to operate for a number of years.

The other instrument type used in this analysis (shown in the right panel in Figure 3) is the Lagrangian float (D'Asaro, 2003), constructed at the University of Washington Applied Physics Laboratory. Two of these instruments were deployed during SPURS-1. Operating mainly in profiling mode, each float sampled the thermohaline structure of the upper ocean for five to six months. A novel buoyancy control system and a set of deployable drogue panels allow the floats to reduce the profiling speed to 5–10 cm s^{-1} near the surface; the slow profiling combined with the 1 Hz sampling rate of the STS unit allows examination of the near-surface

stratification at subdecimeter resolution. Like the APEX floats, the Lagrangian floats carried acoustic sensor units.

THE OBSERVED SPECTRUM OF VARIABILITY

The 16 APEX floats were deployed in September of 2012 in a 200 km × 200 km square, approximately on a grid (Figure 4). The floats were initially parked at depths of 1,000 m and profiled from 2,000 m to the sea surface at 10-day intervals, the canonical Argo sampling protocol. As of late September 2014, two years after

deployment, most of the floats had dispersed out of the initial 200 km square but were still inside the greater SPURS-1 region (a 10° square) depicted in Figures 1 and 2. In an effort to examine near-surface variability on time scales shorter than 10 days, the missions of several of the floats shown in Figure 4 were altered (using Iridium communications) to sample only the upper 200 m of the ocean at two hour intervals; data collected by these floats during this so-called "fast cycling" will form the basis of much of the remaining discussion in this paper.
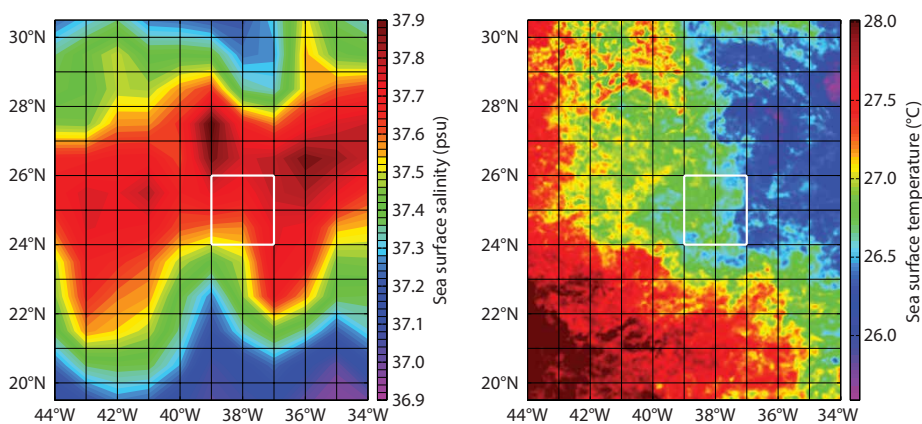

Figure 2. (a) Salinity at the sea surface in the SPURS-1 region of the North Atlantic for September 2013, as measured by the Aquarius/SAC-D satellite. The white square shows the region of the intensive SPURS-1 field program. (b) The Group for High-Resolution Sea Surface Temperature (GHRSST) level-4 global foundation sea surface temperature estimate for the SPURS-1 region for September 15, 2013.

Figure 3. (left panel) An Argo-type APEX profiling float. (middle panel) The upper endcap of an Argo-type APEX profiling float, showing the Iridium antenna, the second surface temperature and salinity sensor (STS) sensor unit (on the white stalk), and the Passive Aquatic Listener (PAL) hydrophone. (right panel) A Lagrangian float being deployed during SPURS-1.

As Figure 5 shows, the observed T/S (temperature/salinity) relation above 10°C based on nearly two years of data from float 7587 (see Figure 4 for the trajectory of this float) provides a good example of the range of variability of temperature and salinity in the upper 700 m or so of this ocean region. At the deepest levels shown, there is only a very thin envelope of possible salinity values at any given temperature, owing to the fact that the waters at this depth have likely not encountered near-surface sources or sinks of T or S for many decades, and weak, ubiquitous background turbulent mixing has had enough time to smooth out any variability generated during these previous encounters with the sea surface. Higher in the water column, at temperatures between about 17°C and 23°C, the salinity envelope widens, reflecting the variability of the properties at the base of the mixed layer in this general region of the ocean. At temperatures above about 23°C, the variability in S at any given T increases substantially, owing to the fact that at these temperatures, the waters are directly ventilated to the atmosphere

during some portion of the annual cycle, with the salinity highly variable, depending on the exact surface conditions at the time of ventilation (e.g., precipitation, evaporation, air temperature, sea state, and wind speed). Investigating this near-surface variability in S has been a central goal of SPURS.

As noted previously, several of the APEX floats deployed during SPURS-1 were put on a fast cycle in order to study the evolution of upper-ocean salinity in detail. In most cases, these fast cycle periods were limited two to three weeks at a time in order to conserve the float batteries. The frequency spectra of temperature and salinity estimated from three weeks of data collected by one fast cycle float, float 7604 in Figure 4, shown in Figure 6, provide a useful picture of the partition of variance across the range of T and S variability sampled by the floats. (The data shown in Figure 6 were collected during one of the few periods in SPURS-1 where there was active, measurable rainfall). Both the T and S spectra are uniformly red (that is, the variance increases from higher to lower frequencies). For

temperature, strong diurnal (~24 hours) and semidiurnal (~12 hours) peaks in the spectrum are present at depths of 0.5 m and 3 m below the sea surface, with weaker but discernible peaks at 10 m. For salinity, very weak peaks at all depths are perhaps present. At frequencies higher than semidiurnal, the T spectra at all three levels, and S spectra at 3 m and 10 m, roll off with the (frequency)$^{-2}$ dependence typical of such spectra at many depths. The S spectrum nearest the sea surface (0.5 m), however, shows evidence of enhanced variance at frequencies higher than semidiurnal.

If upper-ocean temperature and salinity surfaces were simply heaving vertically due to some internal variability, we might expect the T and S spectra to show similar spectral peaks. Yet, while diurnal variability is very prominent in the temperature spectrum close to the sea surface, it is absent near the 24-hour period in the S spectrum. This suggests that at periods near 24 hours, the variability in T is caused by the diurnal cycle of heating at the sea surface; we expect that this cycle in heating would only weakly affect
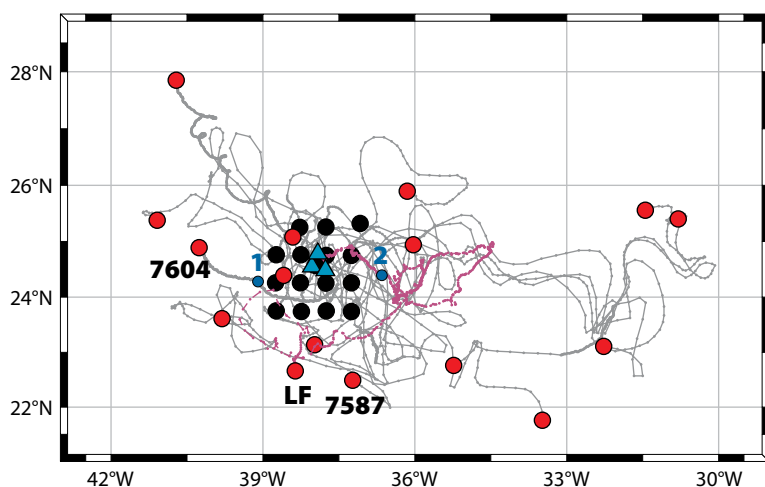

Figure 4. A plot of trajectories of STS-equipped floats and a Lagrangian float deployed as part of SPURS-1 in September 2012. Black circles denote the deployment positions of the floats, and red circles denote their positions on September 1, 2014. The positions of the Lagrangian float and floats 7587 and 7604, discussed in the text, are noted. Trajectories of the STS-APEX floats are noted in gray, and the Lagrangian float trajectory is plotted in magenta. The smaller, numbered blue circles note the positions of rainfall events 1 (from an APEX float) and 2 (from a Lagrangian float) that are discussed in the text.
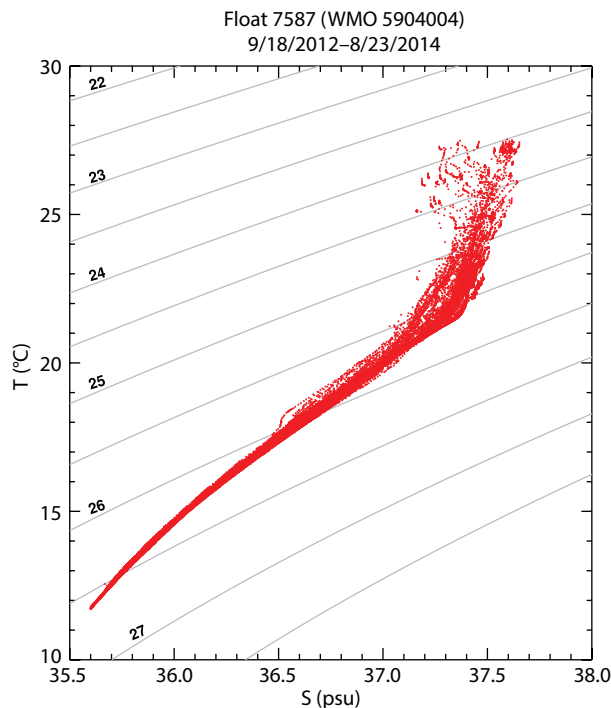

Figure 5. The temperature-salinity (T/S) relation in the SPURS-1 region as measured by float 7587. The curved contours represent σ_t, with the values given along the contours.

near-surface salinity, consistent with the lack of a peak near 24 hours in the S spectra. (Note, however, that at some sites in the global ocean, significant diurnal variability in near-surface S has been observed, as reported by Anderson and Riser, 2014, and Drushka et al., 2014.) At frequencies corresponding to periods near 12 hours, the recognizable peaks in the three T spectra are likely subharmonics of the diurnal warming signal (the diurnal heating is not perfectly sinusoidal, as shown by Gentemann et al., 2003), consistent with the lack of a semidiurnal peak in S.

RAINFALL EVENTS

Evaporation in the SPURS-1 region, averaging nearly 1.5 m yr^{-1} (Schanze et al., 2010; see Figure 1c), greatly exceeds precipitation (about 0.5 m yr^{-1}), accounting in part for the very high surface salinities there, especially in summer. It is difficult to sample the direct effects of evaporation because it is, by definition, a slow, steady loss of water from the sea surface rather than a process composed of discrete events. Precipitation, on the other hand, occurs in discrete events of limited duration, but it is also generally difficult to observe rainfall at sea with high precision. Rainfall was measured at the SPURS-1 central mooring, as discussed by Farrar et al. (2015, in this issue), as well as with floats equipped with passive acoustic sensors, as documented in this issue by Yang et al. (2015). It is occasionally possible to observe the direct effect of rainfall on the sea surface if observational platforms such as floats or gliders are available in the region around the storms. We document here two such events in the SPURS-1 area, the first sampled by one of the 16 APEX floats and the second by a Lagrangian float. It should be noted that there is wide variation in the spatial and temporal scales of precipitation events. As with more familiar terrestrial rainfall events, storms can be hundreds of kilometers in extent and continue for days, or they can be a few kilometers or less in size and last for mere minutes. Given our

sparse sampling of the ocean, even during an intensive measurement program such as SPURS, it is difficult to know much about the scales of the storms that lead to observed upper-ocean salinity changes.

The first oceanic manifestation of a precipitation event was observed in the SPURS-1 region in mid-October 2013 by APEX float 7604 while the float was operating on the fast cycle (see Figure 4 for the trajectory). As shown in the middle panel in Figure 7a, just before local noon on the day preceding the event, the temperature along the float path in the upper few meters of the water column increased until mid-afternoon and then decreased until about 0400 (local time) the following day, roughly in phase with diurnal heating by the sun. At around 0900 (local time) on this second day, however, the upper 3–4 m of the water column rapidly cooled by as much as 0.3°C at a time of day when diurnal heating is rapidly increasing. This cooling persisted

for two to three hours and eventually was mixed downward to a depth of nearly 10 m before the near-surface temperature began to increase, peaking at about 1400 local time. After 1400, the near-surface temperature decreased, seemingly driven by a decrease of solar heating in the afternoon prior to sunset.

The salinity variability associated with these upper-ocean temperature changes suggests the likelihood that a rainfall event occurred in the vicinity of float 7604. As can be seen in the bottom panel of Figure 7a, the salinity was nearly uniform in the upper 10 m of the water column, varying by less than 0.05 psu through the first 20 or so hours shown in Figure 7a. Around 0600 of the second day, the salinity abruptly dropped by 0.35 psu over 1.5 hours (corresponding to the drop in temperature shown in the middle panel of Figure 7a) over the upper 4 m of the water column, with this low-salinity event lasting only about one
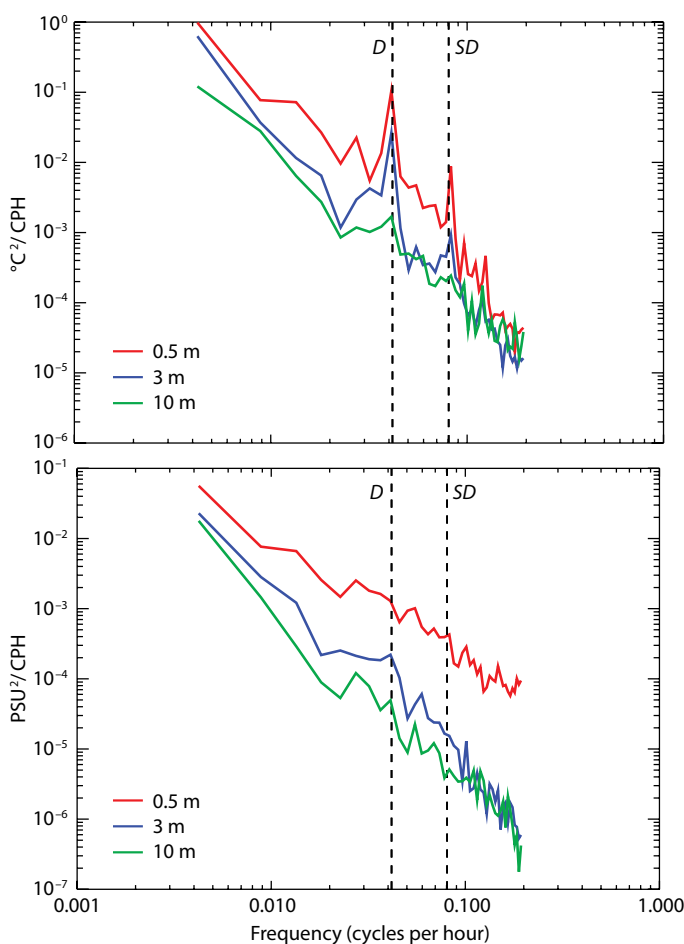

Figure 6. (top panel) The spectrum of near-surface temperature as measured by University of Washington float 7604 in the SPURS-1 region during a three-week period in October of 2013. During this time, the float was profiling from 0–200 m at two-hour intervals. Spectra are shown for depths of 0.5 m, 3 m, and 10 m. The dotted lines denote the diurnal (*D*) and semidiurnal (*SD*) tidal frequencies. (bottom panel) As for the top panel, but for salinity near the sea surface.
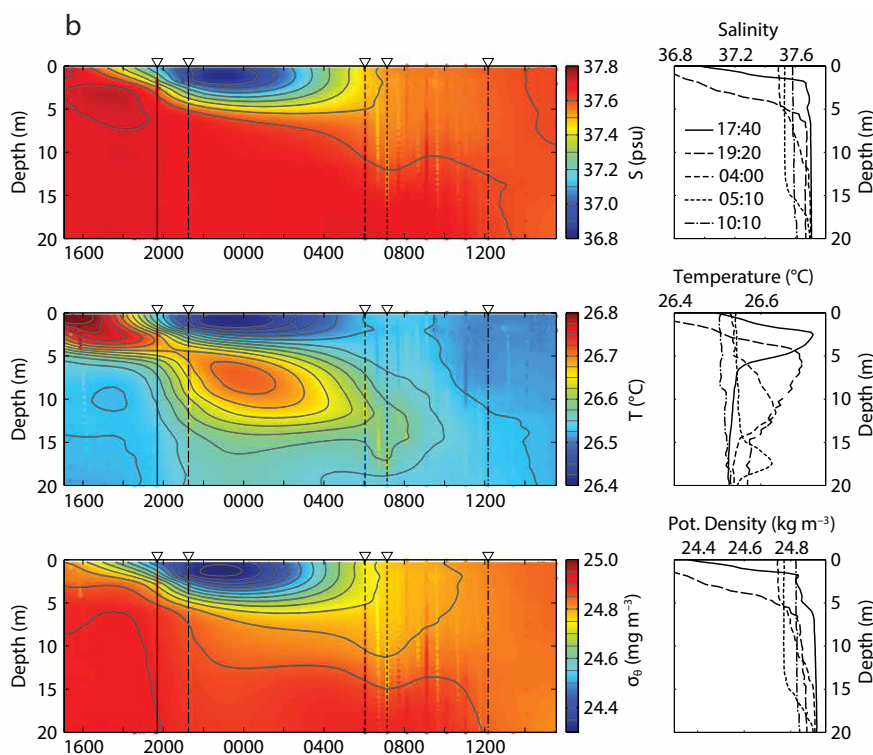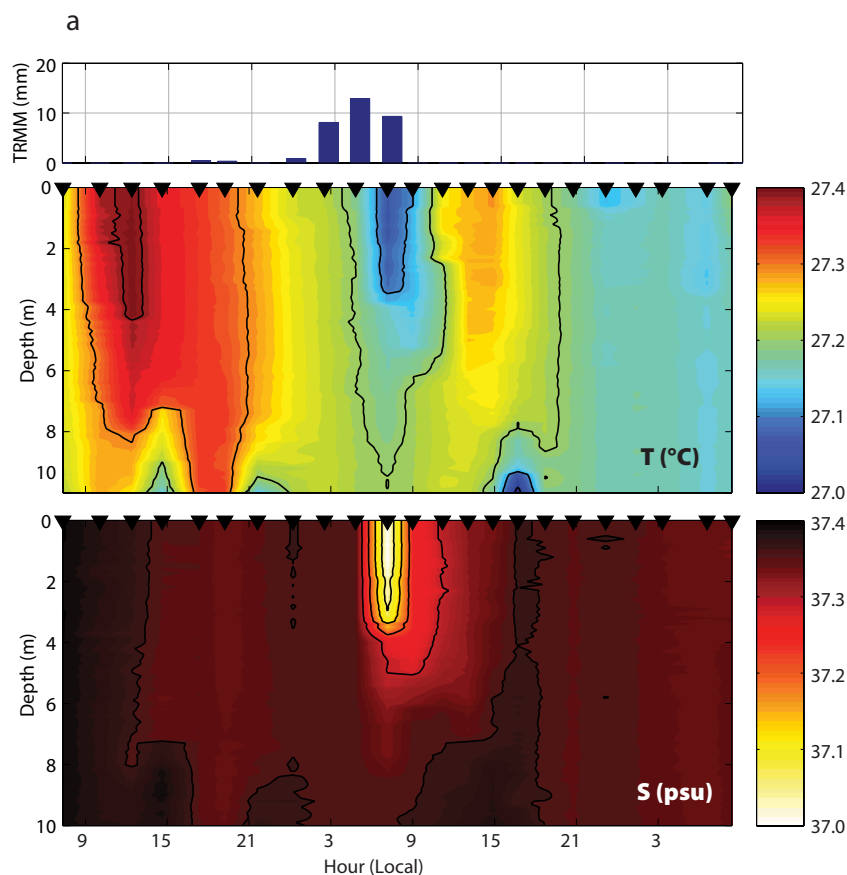
Figure 7. (a) (top panel) Rainfall from the Tropical Rainfall Measuring Mission (TRMM) satellite (data version 3B42), collocated to the position of float 7604. (middle panel) Temperature as a function of local time and depth over the upper 10 m of the water column for October 14 and 15, 2013, as measured by float 7604. The float was sampling from 0–200 m at two-hour intervals. (bottom panel) As for the top left panel, but for near-surface salinity. (b) Rainfall event observed from a Lagrangian float in the SPURS-1 region on October 26, 2012: salinity (top left panel), temperature (middle left panel) and potential density (bottom left panel) over a 24-hour period showing a rainfall event beginning near 2000 local time. (right panels) Evolution of salinity (top), temperature (middle), and potential density (bottom) profiles over this 24-hour period.

hour. A simple calculation shows that the amount of precipitation required to reduce the salinity in this fashion is roughly 44 mm (a sizable fraction of the annual total at this location). As the low salinity mixed downward to a depth of 5–6 m, the salinity returned to its ambient value higher in the water column, and by 1500 local time, the salinity signal from the rainfall event had completely vanished, analogous to the behavior of the temperature variability.

Verification that a precipitation event caused these short-term variations in temperature and salinity can be discerned from the upper panel of Figure 7a, which shows rainfall estimated by the Tropical Rainfall Measuring Mission (TRMM) satellite, interpolated to the space-time location of float 7604. Here, the TRMM 3B42 product has been used; it is available at three-hour intervals on a 25 km grid for this ocean region. The TRMM rainfall estimates indicate an event that lasted about six hours and peaked just prior to the maximum cooling and freshening in the upper few meters of the water column observed by the float. The total amount of precipitation in the event was roughly 40 mm, seemingly consistent with the observed salinity decrease. While the TRMM sampling is coarser than might be desired, it appears clear that the observed temperature and salinity signals were due to a storm of at least several kilometers in horizontal extent, with a lifetime of at least a few hours. Such seemingly minor precipitation events might be quite important in the overall freshwater cycle for this region because the total amount of precipitation associated with this storm (estimated from the upper panel in Figure 7a) is 5–10% of the total annual precipitation, at least locally.

The second precipitation event, observed by one of the Lagrangian floats and depicted in Figure 7b, shows the evolution of a "rain puddle" following a particularly heavy precipitation event on October 26, 2012. The hydrophone on the float registered intermittent heavy rain between 1830 and 2000

local time. The rain gauge on the central mooring (see Figure 4 for the mooring position), located roughly 140 km away from the float, registered maximum precipitation rates of 18 mm hr^{-1}, with an integrated total of 29 mm a few hours later. The wind speed measured at the mooring was 6–8 m s^{-1}, with a brief lull of 2 m s^{-1} during the heaviest rain. Two hours after the end of the rainstorm, the Lagrangian float reported a salinity of 36.8 psu at a depth of 1 m below the surface, a 0.9 psu reduction relative to the pre-rain value. The salinity anomaly decreased linearly with depth, disappearing at a depth of 6 m. This large freshening in the near-surface ocean corresponds to a net input of about 80 mm of precipitation, suggesting the possibility of particularly heavy local precipitation that was not present at the mooring. The downward mixing of the freshwater signature of the puddle continued for the next 20 hours until it was fully incorporated into the 50 m thick surface mixed layer, decreasing the mixed-layer salinity by about 0.1 psu. Following the initial adjustment, the bulk freshwater anomaly stabilized at about 63 mm. The discrepancy with the initial estimate of freshwater input of 80 mm indicates that roughly 20% of the freshwater input might have dispersed via lateral processes.

This storm deposited relatively fresh and cold rainwater on top of the diurnal warm layer. It created peculiar upper-ocean thermohaline stratification with a subsurface temperature inversion, as can be seen in the middle and lower panels of Figure 7b. The overlaying sharp halocline effectively isolated the subsurface temperature maximum from nocturnal convective and wind-driven mixing, allowing it to persist overnight. The maximum was slowly mixed downward over the course of the next 24 hours. Between 0400 and 0900 (local time) on October 27, the vertical position of the maximum fluctuated between 10 and 17 m, suggestive of an internal wave excited at the transient shallow pycnocline (gravitational adjustment of a puddle is potentially a mechanism

for generation of internal gravity waves [Soloviev and Lucas, 1996]). In turn, such a wave may have contributed to the rapid downward mixing of the freshwater anomaly observed during this period.

DIURNAL TEMPERATURE AND SALINITY CYCLES

As an annual average, a solar energy flux of roughly 300 W m^{-2} reaches the sea surface in the SPURS-1 region. This figure is an average of daytime/nighttime values; the absence of solar heating at night leads to a diurnal cycle in temperature at the sea surface, with the day/night difference confined to the upper few meters of the water column in this region (as shown by the depth dependence of the diurnal peak in T in the spectra in Figure 6). The variability at the uppermost levels of the water column is complex and related to surface waves, evaporation and precipitation, atmospheric stirring, and many other effects, in addition to diurnal variability. Thus, observing relatively small, periodic changes in upper-ocean properties over a one-day period presents a challenging observational problem, one with

an uncomfortably small signal-to-noise ratio. To attempt to examine the diurnal cycle, we used data from SPURS-1 float 7604 (see Figure 4 for the trajectory) from the period when the float was sampling on a fast cycle, profiling from 200 m to the sea surface at two-hour intervals. This sampling protocol was in place for approximately three weeks during the autumn of 2013 (the rain event shown in Figure 7a occurred during this period). To reduce noise, temperature, and salinity anomalies (differences from the three-week averages), the upper 5 m of the water column were binned by the local time of day and depth, as the upper panel of Figure 8 shows. When viewed in this way, the diurnal cycle in temperature is clearly evident, with the warmest values (an anomaly in excess of 0.2°C at the sea surface) observed just after local noon and the coolest values (an anomaly of −0.1°C) measured around 0500 in the morning. The warmest values occur in the early afternoon after peak solar insolation (occurring at local noon). The coolest values, however, likely result from a more complicated interplay of weak or
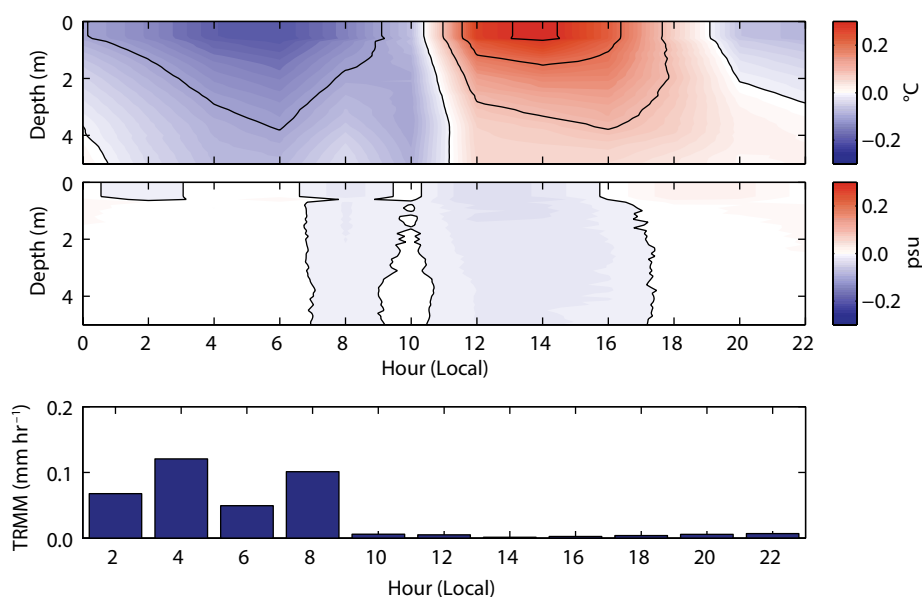

Figure 8. (top panel) The near-surface temperature anomaly (in the upper 5 m of the water column) binned by local time of day for float 7604 during the period it was cycling from 0–200 m at two-hour intervals over a three-week period in October 2013. The mean values over the three-week period were removed. (middle panel) As for the top panel, but for near-surface salinity. (bottom panel) Rainfall from the TRMM satellite, collocated to float 7604 and binned as for temperature and salinity in the upper two panels.

nonexistent insolation, direct loss of heat to the atmosphere (sensible heat loss), and reduced evaporative cooling. There appears to be an observable diurnal cycle to depths of at least 5 m (a downward continuation of the data presented in Figure 8 shows a weak diurnal cycle in T to about 12 m depth). During the cycle's warm-

> **"** As more measurements are made and serve to improve models of these processes, our view of the nature of the distribution of salinity in the upper ocean in particular, and the hydrological cycle in general, will surely improve. **"**

ing phase, the anomaly at the sea surface mixes downward over the course of four to five hours; the stratification during this period is stable, so that wind-generated turbulence mainly drives downward mixing. During the cooling phase, the mixing to 5 m appears to occur somewhat faster, perhaps one to two hours after the minimum temperature at the sea surface; it is likely the cooling of the water at the surface, with uncooled water just below, leads to stratification during this period that is temporarily unstable (a near-surface temperature inversion), producing more-rapid convective overturning.

The analogous diurnal salinity variation (middle panel of Figure 8) is barely discernible, with an amplitude of −0.01 psu just after local noon, probably near the limit of detectability with the STS instrumentation; the anomaly appears to exist to 5 m depth. The weakness of a diurnal signal in salinity is due to the fact that there is no strong evaporation or precipitation-related forcing mechanism at this time scale, unlike the case for diurnal heating. It might be

speculated that warmer temperatures during the daytime should lead to higher evaporation rates (and thus higher salinities), but the change in the saturated water vapor content in the atmosphere due to a diurnal change in atmospheric temperature of 3–5°C is too small to affect the diurnal evaporation rate from

the sea surface (and the surface salinity) by an amount large enough to measure using the STS sensors.

Elsewhere in low-latitude ocean regions, however, measurable diurnal signals in near-surface salinity have been observed (Anderson and Riser, 2014). In these cases, the strong diurnal salinity signal is not closely related to the solar diurnal heating of the surface waters but instead to an observable quasi-diurnal cycle of rainfall; in these regions, significant rainfall occurs around the same time each day, leading to a freshening of the surface waters roughly in phase with the local rainfall. In the Bay of Bengal, for instance, during the southwest monsoon, early afternoon sea surface salinity can be as much as 0.2 psu lower than earlier in the day. Because the effect of rainfall is to increase water column stability, vertical mixing is inhibited during and immediately after the periods of rain. This allows heat to build up in the layer near the sea surface, resulting in a further increase in the stability. In the SPURS-1 region, where evaporation dominates

over precipitation, the diurnal cycle of salinity is much less dramatic. As can be seen in the bottom panel of Figure 8, rainfall during the fast cycling period of float 7604 was quite weak (averaging about 0.5 mm hr^{-1}, mostly between local midnight and 1000 in mid-morning), totaling only a few millimeters over the three-week period, except for the rainfall event shown in Figure 7.

MONTHLY TO ANNUAL VARIABILITY

A plot of temperature and salinity as functions of depth and time along the path of float 7587 (the trajectory is shown in Figure 4) gives an indication of the nature of their variability at time scales of months and longer (Figure 9). Note that for most of its life, this float collected profiles at seven-day intervals; thus, some of the highest frequency variability evident in Figure 9 is likely an artifact of contamination from variability at time scales shorter than the sampling period. However, in general, the spectrum of variability increases so quickly toward lower frequencies that this contamination is likely to be weak in comparison to the variability at periods of weeks and longer. There are seasonal cycles in both T and S (warming of 4–5°C in late summer in the upper 100 m, freshening of 0.3-0.4 psu in the early summer above 50 m). Superimposed upon this seasonality are variations in T and S lasting 50–100 days. This mesoscale eddy variability, generated by modulation of the large-scale gyre or instabilities along frontal regions, can be seen in the map of temperature shown in Figure 2b. Mesoscale eddies are not particularly strong in the SPURS-1 region, as indicated by sea level variance measured by various altimetric satellites that is only about 10% of the values found farther to the northwest in the vicinity of the Gulf Stream (Fu et al., 2010). Yet, although the eddies here are relatively weak, they likely play an important role in stirring the larger-scale salinity and temperature gradients visible in Figure 2 down to smaller spatial scales

(and eventually to the millimeter scale, where true mixing takes place).

A monthly averaged view of the annual cycle (Figure 10) along the path of float 7587 clearly shows warming in late summer and freshening in winter through early summer, with the seasonal cycle confined above depths of 100 m in both temperature and salinity. Figure 10 also shows the depth of the surface mixed layer, which deepens in winter in response to increased wind and weakened thermal stratification, and shallows in late summer, when surface heating is strong and the winds are relatively weak. Late summer is also the time of highest sustained evaporation and smallest precipitation over the year, leading to the highest salinities near the sea surface. One of the ultimate goals of the SPURS-1 experiment was to understand the complete seasonal cycle of salinity near the sea surface in this region; this work is ongoing by SPURS participants, with many of the floats in the region likely to continue to operate for several more years. The effort by both observationalists and modelers to address these questions will likely continue for a number of years before the dynamical and thermodynamical processes involved are well understood.

DECADAL AND LONGER PERIOD VARIABILITY IN SALINITY

Discerning ocean variability at time scales longer than annual is generally difficult, as there are few sites where the multiyear observations necessary for examining such low-frequency variability in detail exist. The international Argo program has provided nearly a decade of global observations of temperature and salinity, and when compared to the observations from previous decades, some initial estimates of regional trends can be made. Roemmich and Gilson (2009) compared global upper-ocean T and S from the early Argo period (2004–2008) with data from the historical record collected through the end of the twentieth century, before Argo began. The comparison showed striking, mapable global patterns of variability on decadal time scales; except for eastern boundary regions, most of the world ocean showed warming in the upper 100 m, sometimes by as much as 1°C, during the time period. The patterns of upper-ocean salinity change were somewhat different: the entire Atlantic was more saline than during the years prior to Argo, by as much as 1 psu in the upper ocean, with much of the Pacific (especially at higher latitudes) fresher by a similar amount. The Roemmich-Gilson estimates for the SPURS-1 region (shown in Figure 11), derived from several thousand shipboard measurements mostly collected in the 1980s and Argo data from 2004–2008, indicate an increase in the near-surface temperature of nearly 0.5°C in the upper 200 m, with weaker warming at most
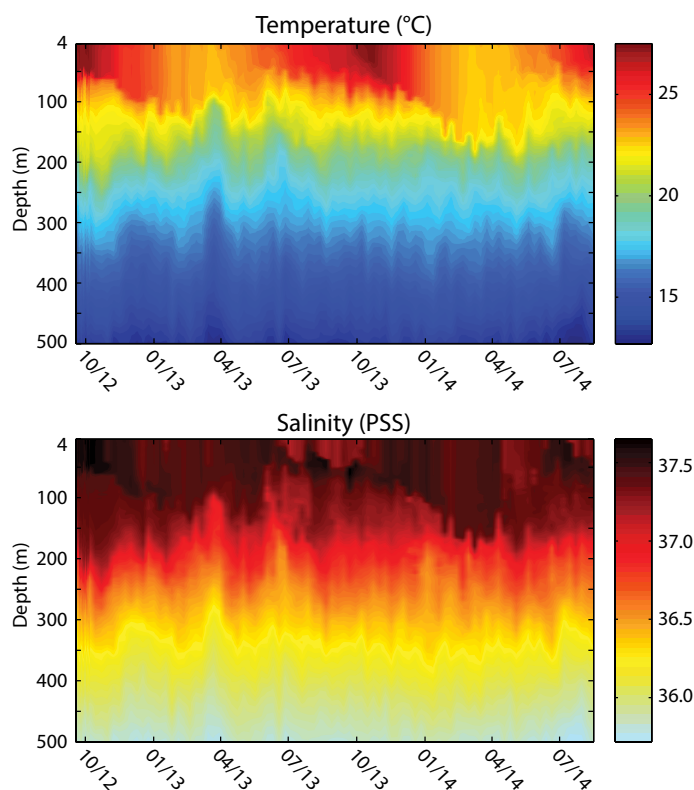

Figure 9. (top panel) Temperature in the upper 500 m from September 2012 through August 2014 along the path of SPURS-1 float 7587. (bottom panel) As for the top panel, but for salinity. The trajectory of float 7587 is shown in Figure 4.
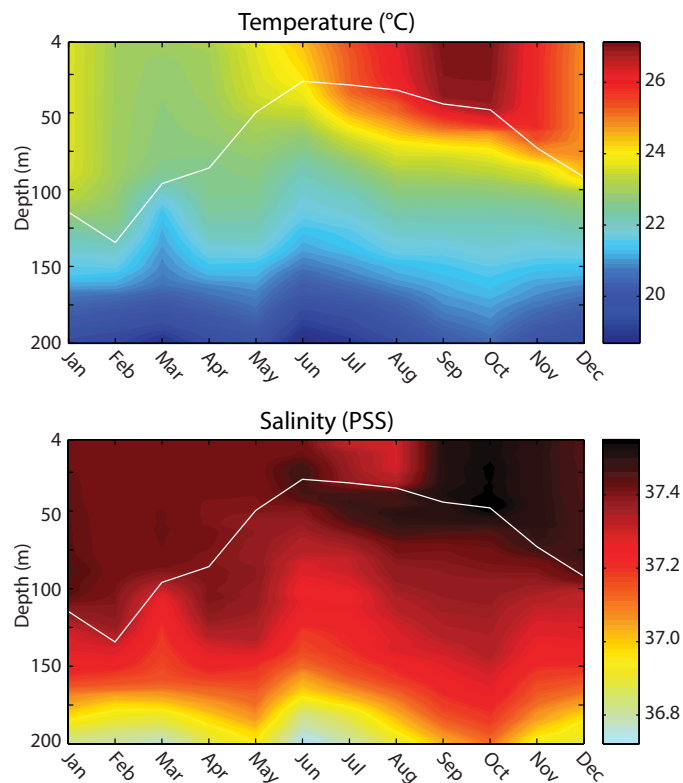
Figure 10. The monthly mean temperature (top panel) and salinity (bottom panel) as a function of depth along the path of float 7587 using data from the period September 2012 through August 2014. The white line shows the depth of the mixed layer based on density.
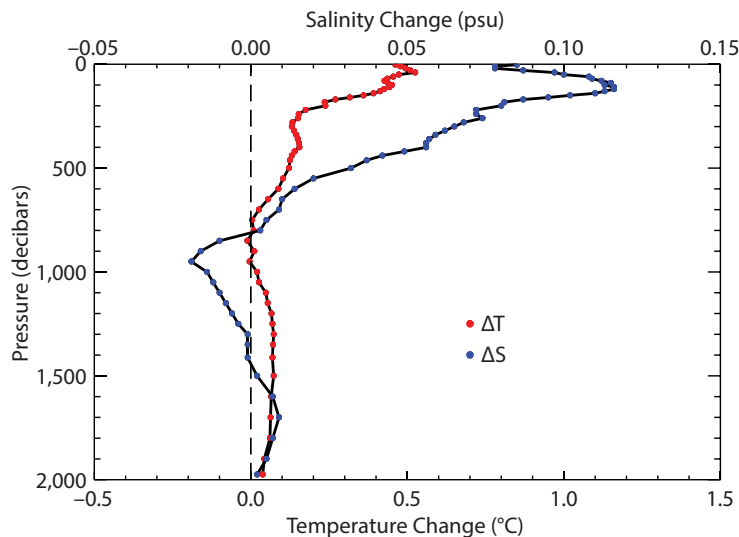
Figure 11. The change in temperature (red dots) and salinity (blue dots) as a function of depth for the SPURS-1 region, estimated as the average of the difference over the region between Argo data for 2004–2008 and data for the region in the World Ocean Atlas 2001; much of the pre-Argo data were collected in the 1980s. These results are similar to those of Roemmich and Gilson (2009). The calculated values for this figure were provided by John Gilson of Scripps Institution of Oceanography.

depths above 2,000 m. Salinity in the upper 200 m increased by as much as 0.12 psu, a seemingly large value nearly comparable in amplitude to the seasonal cycle of salinity (Figure 10). The causes of such changes remain largely unknown.

Durack and Wijffels (2010) examined changes in global sea surface salinity over even longer time scales (50 years), finding changes generally consistent with those found by Roemmich and Gilson (2009). They show that over the past 50 years, surface salinity in the SPURS-1 region has increased more than almost anywhere else in the global ocean. Where surface salinity is presently highest (in the great salinity maxima regions shown in Figure 1b, and especially in the SPURS-1 area), the 50-year positive trends in salinity change are also highest. Where salinity in the world ocean is presently lowest (mostly at high latitudes), the 50-year negative trends in salinity change are also largest, in the negative sense. Such changes are consistent with an overall amplification of the hydrological cycle, with salty regions getting saltier and fresh regions becoming even fresher. As the Argo program continues, more satellite missions such as Aquarius/SAC-D

are launched, and additional local, intensive studies such as SPURS-1 take place at various sites in the world ocean, we should be able to garner a better picture of such long-term trends and, eventually, to understand their causes.

SUMMARY AND CONCLUSIONS

We recall a paper from over 40 years ago (Wunsch, 1972) that examined the thermocline temperature variability near Bermuda on time scales from two minutes to two years. This was one of the first comprehensive studies of the spectrum of a subsurface oceanographic variable over a wide band of frequencies. The short summary we present here is a much less ambitious attempt to do something similar for near-surface salinity, although the dynamical and thermodynamical processes involved here, and the myriad interactions with the atmosphere, are likely more complicated than the adiabatic processes in the deeper ocean. Our results, made possible by collecting some of the first detailed measurements of near-surface salinity over a sizable region for an extended period of time, are largely qualitative, yet in the future, more quantitative studies of this variability will surely

be carried out.

Weak precipitation, weak mean flow, and relatively weak eddies dominate the ocean state in the SPURS-1 region. This relative simplicity was one of the reasons this site was chosen for SPURS-1, and it is hoped that the SPURS-1 effort will lead to a straightforward assessment of the salinity budget for this region. In places where precipitation exceeds evaporation, eddies and wavelike variability are strong, and where there are sizable, strongly sheared mean flows, there will likely be more complicated salinity budgets. It is expected that such regions will be investigated in the near future using experience gained from the SPURS-1 region. The SPURS-1 work demonstrated the value of autonomous platforms such as floats and gliders for carrying out mid-ocean process studies, and ships were used in SPURS-1 mainly for deployment and recovery of these assets, at a great cost savings.

The thermohaline sources and sinks for the ocean occur at large spatial scales; the equator-to-pole temperature gradient sets the scale of thermal forcing, and the pattern of evaporation minus precipitation as shown in Figure 1c sets the scale for surface salinity. Thus, the scales of variation near the sea surface are large. This variance must be removed by mixing at millimeter scales. As the variance moves from large scales to small, it manifests as geostrophic eddies, diurnal variability, internal gravity waves, and smaller, unsampled phenomena; the addition of rain pools derived from local storms adds to salinity variance in the submesoscale range. Our objective here has been to provide a simple description of some new observations of these processes. As more measurements are made and serve to improve models of these processes, our view of the nature of the distribution of salinity in the upper ocean in particular, and the hydrological cycle in general, will surely improve. ◎

REFERENCES

Anderson, J., and S. Riser. 2014. Near-surface variability of temperature and salinity in the near-tropical ocean: Observations from profiling floats. *Journal of Geophysical Research* 119:7,433–7,448, http://dx.doi.org/10.1002/2014JC010112.

D'Asaro, E. 2003. Performance of autonomous Lagrangian floats. *Journal of Atmospheric and Oceanic Technology* 20:896–911, http://dx.doi.org/10.1175/1520-0426(2003)020<0896:POALF>2.0.CO;2.

Drushka, K., S. Gille, and J. Sprintall. 2014. The diurnal salinity cycle in the tropics. *Journal of Geophysical Research* 119:5,874–5,890, http://dx.doi.org/10.1002/2014JC009924.

Durack, P., and S. Wijffels. 2010. Fifty-year trends in global ocean salinities and their relationship to broad-scale warming. *Journal of Climate* 23:4,342–4,362, http://dx.doi.org/10.1175/2010JCLI3377.1.

Farrar, J.T., L. Rainville, A.J. Plueddemann, W.S. Kessler, C. Lee, B.A. Hodges, R.W. Schmitt, J.B. Edson, S.C. Riser, C.C. Eriksen, and D.M. Fratantoni. 2015. Salinity and temperature balances at the SPURS central mooring during fall and winter. *Oceanography* 28(1):56–65, http://dx.doi.org/10.5670/oceanog.2015.06.

Fu, L.-L., D. Chelton, P.-Y. LeTraeon, and R. Morrow. 2010. Eddy dynamics from satellite altimetry. *Oceanography* 23(4):14–25, http://dx.doi.org/10.5670/oceanog.2010.02.

Gentemann, C., C. Donlon, A. Stuart-Menteth, and F. Wentz. 2003. Diurnal signals in satellite sea surface temperature measurements. *Geophysical Research Letters* 30, 1140, http://dx.doi.org/10.1029/2002GL016291.

Gray, A., and S. Riser. 2014. A global analysis of Sverdrup balance using absolute geostrophic velocities from Argo. *Journal of Physical Oceanography* 44:1,213–1,229, http://dx.doi.org/10.1175/JPO-D-12-0206.1.

Riser, S.C., J. Nystuen, and A. Rogers. 2008. Monsoon effects in the Bay of Bengal inferred from profiling float-based measurements of wind speed and rainfall. *Limnology and Oceanography* 53:2,080–2,093, http://dx.doi.org/10.4319/lo.2008.53.5_part_2.2080.

Roemmich, D., and J. Gilson. 2009. The 2004–2008 mean and annual cycle of temperature, salinity, and steric height in the global ocean from the Argo program. *Progress in Oceanography* 82:81–100, http://dx.doi.org/10.1016/j.pocean.2009.03.004.

Schanze, J., R. Schmitt, and L. Yu. 2010. The global oceanic freshwater cycle: A state-of-the-art quantification. *Journal of Marine Research* 68:569–595, http://dx.doi.org/10.1357/002224010794657164.

Soloviev, A., and R. Lukas. 2006. *The Near-Surface Layer of the Ocean: Structure, Dynamics, and Applications*. Springer, 572 pp.

Wunsch, C. 1972. The spectrum from two years to two minutes of temperature variability in the main thermocline at Bermuda. *Deep Sea Research* 19:577–593, http://dx.doi.org/10.1016/0011-7471(72)90041-1.

Yang, J., S.C. Riser, J.A. Nystuen, W.E. Asher, and A.T. Jessup. 2015. Regional rainfall measurements using the Passive Aquatic Listener during the SPURS field campaign. *Oceanography* 28(1):124–133, http://dx.doi.org/10.5670/oceanog.2015.10.

AUTHORS. **Stephen C. Riser** (riser@ocean.washington.edu) is Professor, School of Oceanography, University of Washington, Seattle, WA, USA. **Jessica Anderson** is a graduate student in the School of Oceanography, University of Washington, Seattle, WA, USA. **Andrey Shcherbina** is Senior Oceanographer, Applied Physics Laboratory, University of Washington, Seattle, WA, USA. **Eric D'Asaro** is Senior Principal Oceanographer, Applied Physics Laboratory, and Professor of Oceanography, University of Washington, Seattle, WA, USA.